Reaction with Mole Changes in Porous Catalysts in the Molecular, Transition, and Knudsen Regimes

Equations are derived and solved numerically for the intrapellet pressure and composition profiles in porous catalysts. The extended dusty-gas model is used to describe the transport for a zero-order, irreversible reaction with mole changes. Results agree with other models in the purely Knudsen and molecular regimes. In the transition region, however, the effectiveness factor is a function of five dimensionless parameters. The calculations predict a significant pressure gradient in the Knudsen regime and transition region but an insignificant gradient in the molecular regime for reactions with mole changes. Since many industrial catalysts operate in the transition region of transport, these calculations are highly desirable in reactor design.

RAN ABED and ROBERT G. RINKER

Department of Chemical and Nuclear Engineering
University of California
Santa Barbara, California 93106

SCOPE

This study was undertaken to show how the effectiveness factors of slab, cylindrical, and spherical catalyst pellets behave in the transition region of mass transport for isothermal, zero-order reactions with mole changes. Since this region includes contributions from both molecular and Knudsen flow phenomena, the extended dusty-gas model for transport was used in a numerical study to determine the parametric dependencies of the effectiveness factor.

Previous work had dealt with only purely molecular or purely Knudsen flow in porous catalysts where analytical as well as numerical techniques were used. Those investigators found a unique dependence of the effectiveness factor on the Knudsen Thiele parameter in the Knudsen regime and a dependence on both the molecular Thiele parameter and a volume-change parameter in the molecular regime. No one has previously studied the effectiveness factor behavior in the transition region.

Since many industrial catalysts operate in the transition region, this type of study is considered essential in tying together previous studies on both sides in addition to identifying and understanding the characteristics of the parameters which must be specified to obtain a valid effectiveness factor in the transition region.

CONCLUSIONS AND SIGNIFICANCE

The extended dusty-gas model was chosen primarily for its correctness in describing mass transport in the transition region. Also of importance, however, is the fact that it contains three easily determined constants C_0, C_1 and C_2 which are dependent only on the structure of the porous catalyst. These constants are obtained experimentally but do not require pore-size distribution measurements.

The numerical studies show that the effectiveness factor in the transition region is dependent on five dimensionless parameters, namely, a pressure parameter α, a flow parameter β, a mole change parameter θ, the molecular Thiele parameter γ_M, and finally an external-composition parameter y_{AL}. In the Knudsen and molecular regimes, on each side of the transition region, the parametric dependencies completely agree with the results of previous investigators.

The study also shows that extension of the simpler Knudsen and molecular models into the transition region can result in considerable error in estimating the effectiveness factor for certain value ranges of the parameters. Use of the extended dusty-gas model in describing mass transport in porous catalysts thus allows the reactor designer to obtain correct effectiveness factors over the entire range of transport regimes.

This study generalizes the characterization of mass transport in porous catalysts and provides continuity to previous results.

The effects of intraparticle transport on the kinetics of reaction in porous catalysts can be described in terms of the effectiveness factor concept. For isothermal systems in which there are no mole changes and in which the transport of reactants and products in the porous catalyst is governed either by ordinary molecular diffusion or by Knudsen diffusion, previous investigators (Aris, 1957; Bischoff, 1965; Smith and Amundson, 1951; Thiele, 1939; Wakao and Smith, 1964; Wei, 1962; Weisz and Prater, 1954; Wheeler, 1951) have found a unique dependence of the effectiveness factor on the Thiele modulus. Exact analytical expressions for the dependence of the effectiveness factor on the Thiele modulus have been obtained for zero and first-order reactions on slabs, cylinders, and spheres (Aris, 1957; Wei, 1962; Wheeler, 1951). Higher-

Correspondence concerning this paper should be addressed to R. G. Rinker.

order reactions have required numerical methods. A concise review of these studies appears elsewhere (Weekman and Gorring, 1965).

For systems in which mole changes occur and in which the transport of reactants and products is by ordinary molecular diffusion, the effectiveness factor has been shown to be dependent not only on the Thiele modulus but also on a volume-change parameter (Lin and Lih, 1971; Weekman and Gorring, 1965), which contains both the stoichiometric factor describing mole changes and the mole fraction of the reactant on the external surface of the pellet. Exact analytical expressions have been obtained for zero-order reactions with mole changes on the three main geometries (Lin and Lih, 1971). Higher-order reactions on all three geometries have been treated numerically over wide ranges of values for the two parameters (Weekman and Gorring, 1965); and for large values of the Thiele modulus, asymptotic analytical solutions were obtained. These served as a check on the numerical results.

When Knudsen diffusion predominates in systems with mole changes, it has been shown that the effectiveness factor again becomes a function of only the Thiele modulus, even though a significant intrapellet pressure gradient can develop (Otani et al., 1964).

Previous studies have restricted the intrapellet transport to either ordinary molecular diffusion or to Knudsen diffusion. Essentially no one has dealt with the problem of generalizing the effectiveness factor concept to include Knudsen, transition, and ordinary molecular diffusion regimes wherein the variations of effective diffusivity with composition and pressure are taken into account.

Commercial solid catalysts usually contain a random and tortuous arrangement of pores which may vary in size from several microns down to a few angstroms within the same particle. At a given operating pressure and temperature, the tortuous movement of reactants and products may be in any one of the three transport regimes throughout the pellet or in all three at the same time. A general model which takes into account the pore geometry as well as the transport regime is required.

The dusty-gas model is particularly attractive because, in the transition region, it correctly combines the simultaneous effects of ordinary molecular diffusion and Knudsen diffusion in any general array of pores (Evans et al., 1961). Furthermore, the model reduces to the correct limiting forms under restricted conditions. To account for flow fluxes resulting from a pressure gradient, a D'Arcy flow term can be added (Gunn and King, 1969; Mason et al., 1967). When the D'Arcy term is included, the extended model contains three measurable constants which account for the effects of pore geometry and distribution on the transport of ordinary gaseous molecules. Several other models are currently in use but are not as theoretically well founded as the extended dusty-gas model. These are adequately reviewed elsewhere (Youngquist, 1970).

It is the objective of this paper, therefore, to show the effects of mole changes, pellet geometry, and the transport regime on the kinetics of zero-order reactions in porous catalysts. The paper is restricted to zero-order reactions because of their unique behavior relative to other orders. For an irreversible zero-order reaction wherein the rate is independent of concentration, the effectiveness factor simply becomes the ratio of the volume of pellet occupied by reactant to the entire pellet volume. By this definition, the effectiveness factor is always unity until the depth at which reactant concentration goes to zero is less than the overall radius or half-thickness of the pellet.

In using the extended dusty-gas model to describe transport in the transition region, the effectiveness factor is no longer a function of only two parameters as it is in the molecular regime but, as will be shown, five dimensionless parameters. Since the equations cannot be solved analytically, numerical methods are used to obtain generalized plots for the zero-order reaction case. It is of interest to note that this general treatment gives the same results obtained by previous investigators in the Knudsen and ordinary molecular regimes. By taking into account the transition-region transport, it is our opinion that previous restrictions on the use of the effectiveness factor concept are eliminated.

THEORY

The mass transport equation of diffusion and flow in porous media has been derived by Mason et al. (1967) and independently by Gunn and King (1969). The equation contains three parameters C_0, C_1, C_2 which characterize the porous medium and must be determined experimentally. Using the notation of Gunn and King (1969), the equation for a binary system of A and B is as follows:

$$\vec{N}_A = -\frac{C_2 D^0_{AB} K_A P}{(C_2 D^0_{AB} + K_m P)\, R_g T} \nabla y_A - \left[\frac{K_A (C_2 D^0_{AB} + K_B P)}{C_2 D^0_{AB} + K_m P} + \frac{C_0 P}{\mu_m}\right] \frac{y_A}{R_g T} \nabla P \quad (1)$$

When applied to a one-dimensional system of porous catalyst as shown in Figure 1, Equation (1) becomes

$$\overleftarrow{N}_A = a \frac{dy_A}{dZ} + b \frac{dP}{dZ} \quad (2)$$

where "a" and "b" are given by

$$a = \frac{C_2 D^0_{AB} K_A P}{(C_2 D^0_{AB} + K_m P)\, R_g T} \quad (3)$$

$$b = \left[\frac{K_A (C_2 D^0_{AB} + K_B P)}{C_2 D^0_{AB} + K_m P} + \frac{C_0 P}{\mu_m}\right] \frac{y_A}{R_g T} \quad (4)$$

The flux of species B can be described similarly by

$$\vec{N}_B = -a' \frac{dy_B}{dZ} - b' \frac{dP}{dZ} \quad (5)$$

where a' and b' are given by the relationships

$$a' = \frac{C_2 D^0_{AB} K_B P}{(C_2 D^0_{AB} + K_m P)\, R_g T} \quad (6)$$

$$b' = \left[\frac{K_B (C_2 D^0_{AB} + K_A P)}{C_2 D^0_{AB} + K_m P} + \frac{C_0 P}{\mu_m}\right] \frac{y_B}{R_g T} \quad (7)$$

If species A and B participate in a chemical reaction scheme with the following overall stoichiometry:

$$A \rightarrow \theta B$$

the induced flux ratio n becomes

$$n = \frac{\vec{N}_B}{\vec{N}_A} = -\frac{M_A}{M_B} \quad (8)$$

For the case where $y_A + y_B = 1$, we obtain

$$\frac{dy_A}{dZ} = -\frac{dy_B}{dZ} \quad (9)$$

Combining Equations (2), (5), (8), and (9) gives us a relationship between the gradients of composition and pressure; that is,

$$\frac{dP}{dZ} = \left(\frac{na + a'}{b' - nb}\right)\frac{dy_A}{dZ} \tag{10}$$

Combination of Equations (2) and (10) then allows us to solve for $\overleftarrow{N}_A$ as a function of the concentration derivative; that is,

$$\overleftarrow{N}_A = f\left(\frac{dy_A}{dZ}\right) \tag{11}$$

where f is given by

$$f = a + b\left(\frac{na + a'}{b' - nb}\right) \tag{12}$$

A steady state molar balance for a zero-order, irreversible reaction in the three main geometries is as follows:

$$\frac{d\overleftarrow{N}_A}{dZ} + \frac{(j-1)\,\overleftarrow{N}_A}{Z} = \rho_p S k' = k \tag{13}$$

where $j = 1$, 2, and 3 for an infinite slab, cylinder, and sphere, respectively. The boundary condition is simply

$$\text{at} \quad Z = Z_0, \quad \overleftarrow{N}_A = 0 \tag{14}$$

Integration of Equation (13) and substitution of the boundary condition gives

$$\overleftarrow{N}_A = \frac{k}{j}\left(Z - \frac{Z_0^j}{Z^{j-1}}\right) \tag{15}$$

Substituting Equation (15) into Equation (11) gives the final working equation for the intrapellet composition profile in dimensional form; that is,

$$\frac{dy_A}{dZ} = \frac{k}{jf}\left(Z - \frac{Z_0^j}{Z^{j-1}}\right) \tag{16}$$

Combining Equations (10) and (11) and substitution for $\overleftarrow{N}_A$ from Equation (15) gives the final working equation for the intrapellet pressure profile in dimensional form; that is,

$$\frac{dP}{dZ} = \frac{k}{j}\left(Z - \frac{Z_0^j}{Z^{j-1}}\right) \Big/ \left[\frac{a(b' - nb)}{na + a'} + b\right] \tag{17}$$

Equations (16) and (17) can now be nondimensionalized and subsequently solved numerically.

The nondimensionalization produces five main parameters which can be described as follows:

$$\alpha = \frac{K_A P_L}{C_2 D^0{}_{AB}} \tag{18}$$

$$\beta_0 = \frac{C_0 C_2 D^0{}_{AB}}{\mu_m \sqrt{\theta}\, K_A{}^2} \tag{19}$$

$$\gamma_M = L\left(\frac{k R_g T}{y_{A_L} C_2 D^0{}_{AB}}\right)^{1/2} \tag{20}$$

$$\theta = \frac{M_A}{M_B} \tag{21}$$

The fifth parameter is y_{A_L}, the mole fraction of species A at the outside pellet surface, where $Z = L$.

Two useful auxiliary parameters are defined as follows:

$$\gamma_K = \gamma_M/\alpha^{1/2} \tag{22}$$

$$\beta = \beta_0 \alpha \tag{23}$$

The dependent and independent variables can also be nondimensionalized and are listed below.

$$Y = \frac{y_A}{y_{A_L}} \tag{24}$$

$$X = \frac{Z}{L} \tag{25}$$

$$X_0 = \frac{Z_0}{L} \tag{26}$$

$$\xi = \frac{P}{P_L} \tag{27}$$

Equations (16) and (17), written in dimensionless form followed by considerable algebraic manipulation, then become

$$\frac{dY}{dX} = R\,(X - X^*)/j \tag{28}$$

and

$$\frac{d\xi}{dX} = QR\,(X - X^*)/j \tag{29}$$

where X^* is defined for the different pellet geometries as follows:

$$X^* = X_0{}^j/X^{j-1} \tag{30}$$

In Equations (28) and (29), Q and R are the lumped dependent variables and are given by the expressions

$$Q = (1 - \sqrt{\theta})\, y_{A_L}\xi/W \tag{31}$$

$$R = \gamma^2 \Big/ \left\{ \frac{\xi}{V} + \frac{\xi(1-\sqrt{\theta})}{W}\left[\frac{(1 + \sqrt{\theta}\,\alpha\,\xi)\, Y\, y_{A_L}}{V} + \sqrt{\theta}\,\beta\xi Y\, y_{A_L}\right]\right\} \tag{32}$$

The groupings V and W appearing in Q and R are further defined as follows:

$$V = 1 + (1 - Y\, y_{A_L})\,\alpha\,\xi + \sqrt{\theta}\,\alpha Y\, y_{A_L}\xi \tag{33}$$

$$W = (1 - Y\, y_{A_L})(1 + \alpha\xi) + \sqrt{\theta}\,(1 + \sqrt{\theta}\,\alpha\xi)\, Y\, y_{A_L} + V[\theta\beta\xi Y\, y_{A_L} + \beta\xi(1 - Y\, y_{A_L})] \tag{34}$$

Finally, the effectiveness factor for this zero-order reaction and for the three pellet geometries becomes

$$E = 1 - X_0{}^j \tag{35}$$

RESULTS

The numerical integration of the dimensionless equations (28) and (29) was accomplished with a fourth-order, Runge-Kutta integration formula. In each case, values of the five main parameters α, β_0, γ_M, θ, and y_{A_L} were chosen for a particular geometry. The integration was started by guessing a value of X_0 for which $Y = 0$ and then integrating from the outer surface of the pellet where $\xi = 1$ and $Y = 1$. The value of X_0 was adjusted by an iterative process until the condition of $Y = 0$ at X_0 was satisfied to within an error limit of plus or minus one part in 10^{+7}.

The ranges of values used for the five main parameters are listed in Table 1. Values of the auxiliary parameters γ_K and β depend by definition on the main parameters; their ranges are listed in Table 2.

The parameter α is primarily a measure of the influence

Table 1. Ranges of Values for the Main Parameters

Parameter	Range of study: Lower limit	Range of study: Upper limit
α	10^{-8}	10^{+8}
β_0	10^{-2}	10^{+2}
γ_M	10^{-1}	8
Θ	1	4
y_{AL}	1	1

Table 2. Ranges of Values for the Auxiliary Parameters

Parameter	Calculated range: Lower limit	Calculated range: Upper limit
γ_K	10^{-5}	8×10^{4}
β	10^{-10}	10^{+10}

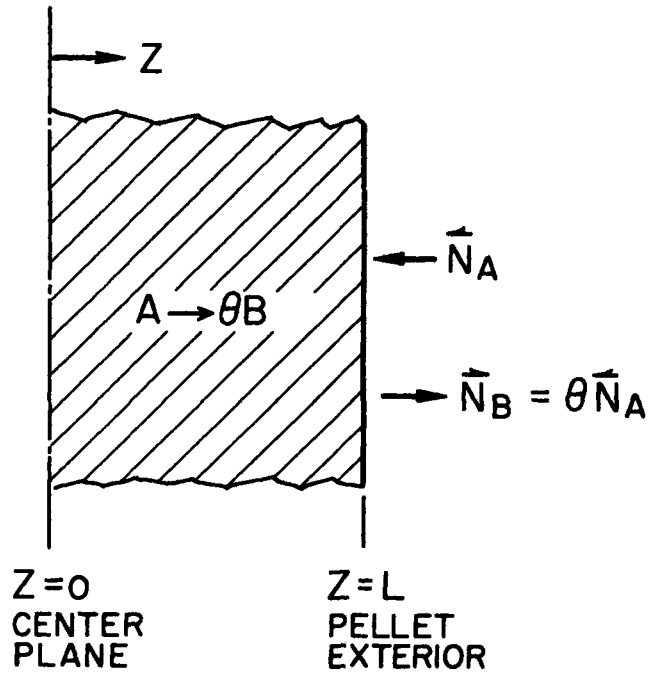

Fig. 1. Coordinate and flux directions in one-dimensional catalyst pellet.

of the operating pressure level. By varying α over a 10^{16}-fold range, the entire transition region is traversed along with deep penetration into the Knudsen and ordinary molecular regimes of transport. In fact, the transition region is completely bracketed with $10^{-4} < \alpha < 10^{4}$. The value of this pressure parameter is therefore a very useful criterion for locating the region of transport in a given system.

The relative effects of slip and D'Arcy flow are indicated by the flow parameter β_0. For small values of β_0, slip flow dominates over D'Arcy flow and vice versa. A 10^4-fold variation in β_0 was sufficient to completely determine its effects on transport behavior in the pellets. For uniform external pressure, it was also found that β_0 influences intrapellet transport only in the transition region, which lies between the limits of α listed above.

The parameter γ_M is the molecular Thiele modulus defined in terms of the molecular diffusivity and is often called the kinetic-diffusion parameter. Its range of values, given in Table 1, includes those normally expected for commercial catalysts.

Changes in moles or volume due to reaction are reflected by the parameter θ. The choice of the seemingly narrow range of values for this mole-change parameter is again governed by practical considerations. Mole changes higher than those listed in Table 1 are possible but generally are not very common in practice. Values of θ less than unity are found in practice but were not considered in this paper for reasons of brevity.

Although the external-composition parameter y_{AL} normally varies in batch and tubular reactors and may even vary around a single pellet, its value was held constant at unity throughout our study. This was a reasonable approach, since our main interest was to study behavior inside the pellet, especially when conditions for transition flow are dominant.

In presenting the results of the numerical integration, we have attempted to selectively show in graphical form the important effects of the main parameters on the intrapellet pressure profiles and on pellet effectiveness factors. Other combinations of the parameters and variables could be used, but we feel that our choices will best fit the needs of the user. Our equations and computer program are sufficiently general so that one can generate plots for conditions not represented by the curves in Figures 2 through 7.

Figure 2 shows the intrapellet pressure profiles in slab geometry ($j = 1$) for the three regions of transport. The values of α were chosen to be 0.5×10^{-4}, 0.1, and 1×10^{6} for the Knudsen, transition, and molecular regions, respectively. The mole change by reaction, corresponding to $\theta = 4$, represents more-or-less a practical upper limit. Since an effectiveness factor of $E = 0.5$ was used in Figure 2, the reactant penetrates only to a dimensionless depth of $X = 0.5$. The values of the molecular Thiele modulus γ_M required to give the fixed value of $E = 0.5$ are 0.7687 and 1.923 for the transition and molecular regions, respectively. Likewise the value of the Knudsen Thiele modulus γ_K is 2.828 for the Knudsen regime. The parameter β_0 is held constant at 1.0, which corresponds to a value considered to be typical

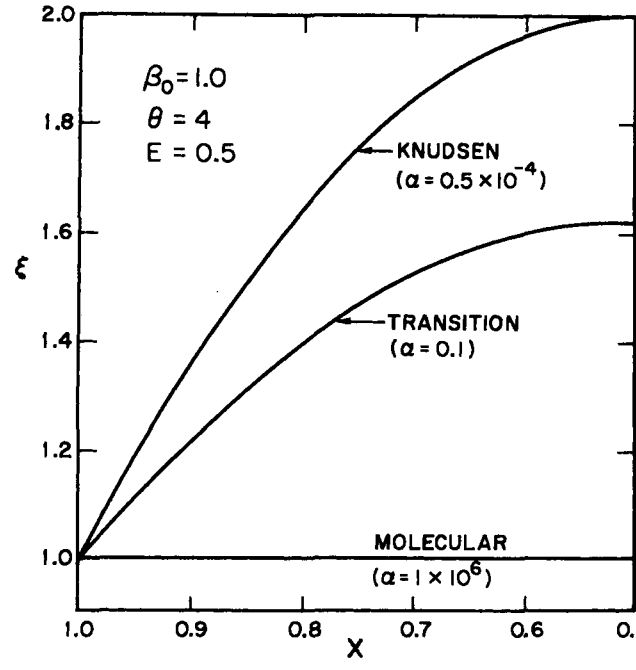

Fig. 2. Pressure gradients in slab geometry for $\gamma_M = 1.923$ in molecular regime, $\gamma_M = 0.7687$ in transition region, and $\gamma_K = 2.828$ in Knudsen regime.

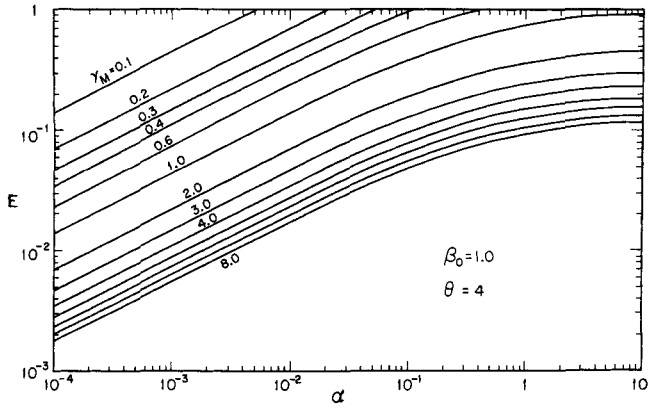

Fig. 3. Effectiveness factor in the transition region for slab geometry, showing the effects of the Thiele modulus.

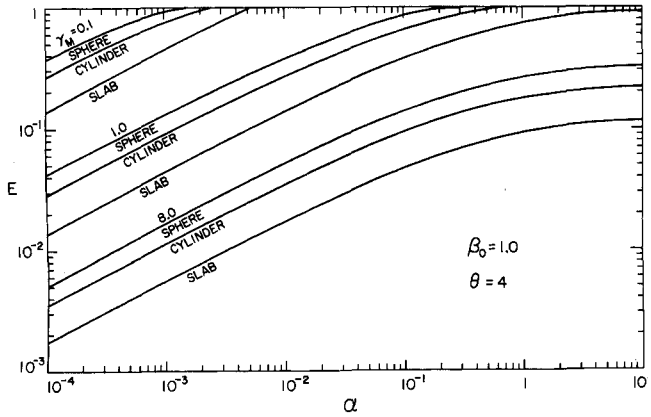

Fig. 4. Effectiveness factor in the transition region for different Thiele moduli showing the effects of geometry.

for practical applications.

Figures 3 and 4 show the variation of the effectiveness factor with the pressure parameter α in the transition region. Both figures use the same values of $\beta_0 = 1.0$ and $\theta = 4$. The molecular Thiele modulus is varied over a range of 0.1 to 8, which includes those values normally expected for commercial catalysts. As expected, an increase in the Thiele modulus causes a decrease in E. Our results also show that, in this important region, the effectiveness factor is a function of all five of the main parameters; and the effects of two of them are observed here.

The effectiveness-factor curves in Figure 3, for slab geometry, reach the limiting value of $E = 1$ asymptotically for γ_M near unity; but as γ_M becomes smaller, the curves reach the limiting value discontinuously. This behavior is unique for zero-order reactions. For γ_M larger than unity, the curves become asymptotic to values $E < 1$ as α increases. This asymptotic behavior is expected, since α is approaching values associated with the molecular regime. In that regime, we know that E is independent of α for fixed values of γ_M, θ and y_{AL}. Similar behavior is shown for the cylindrical and spherical pellet in Figure 4 except that the value of γ_M, for which the curves reach $E = 1$, increases. The curves in each figure are purposely terminated at the lower limit of $\alpha = 10^{-4}$ because, as noted previously, the Knudsen regime dominates at lower values of α. In that regime the γ_M and α can be replaced by γ_K since E is uniquely dependent on γ_K.

In Figure 5, the effectiveness factor in the transition region for slab geometry ($j = 1$) is again shown. Here, however, the effects of varying θ from 1 to 4 are observed for $\beta_0 = 1.0$. Increasing θ causes a decrease in the effectiveness factor in the transition region. As α approaches the Knudsen region, however, the mole-change effect vanishes as each set of curves converges to a single one; but as α approaches the molecular region, there is significant divergence, especially near $\gamma_M = 1$. It is also interesting to note that the divergence is less pronounced on either side of $\gamma_M = 1$. Again, as previously noted for $\gamma_M < 1$, the effectiveness-factor curves discontinuously reach the limit of $E = 1$; but for $\gamma_M > 1$, the curves again reach asymptotic values of $E < 1$. Similar behavior of the effectiveness factor occurs in the other two geometries.

Thus far, we have observed the dependence of the effectiveness factor in the transition region on α, γ_M, and θ. Since we are keeping y_{AL} constant throughout the study, it only remains to see the effect of β_0. Figure 6 shows for slab geometry and for $\theta = 4$ that, only in the transition region, does β_0 influence the effectiveness factor. With β_0 varying over a 10^4-fold range, the variation of E is relatively small but cannot be neglected, especially for $\gamma_M \leq 1$. For values of β_0 outside the range indicated, the variation of E is insignificant. Similar behavior of the effectiveness factor occurs for the other two geometries.

DISCUSSION AND CONCLUSIONS

By analyzing the effects of mole changes on the coupled mass transport and chemical reaction in catalyst pellets for the transition region as well as for the molecular and Knudsen regimes, we have eliminated restrictions on the use of the effectiveness factor concept. Our results for the molecular and Knudsen regimes of transport using the dusty-gas model agree exactly with analytical as well as numerical studies of others (Lin and Lih, 1971; Otani, et al., 1964; Weekman and Gorring, 1965). To our knowledge, however, effectiveness-factor behavior in the transition region has not been previously published.

In the discussion which follows, useful generalizations are stated; and in doing so, it is convenient to treat each transport regime separately.

Molecular Regime

In agreement with others (Lin and Lih, 1971; Weekman and Gorring, 1965) the effectiveness factor depends only on the molecular Thiele modulus γ_M and on a volume-change parameter $(\theta - 1)y_{AL}$. For intrapellet transport

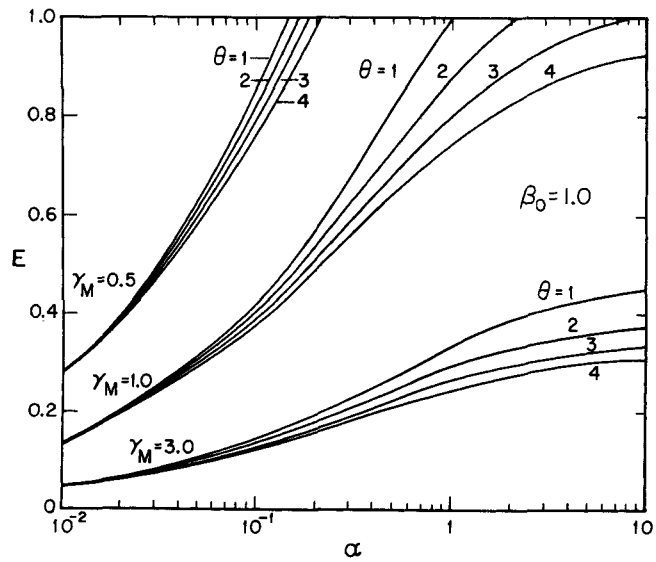

Fig. 5. Effectiveness factor in the transition region for slab geometry showing the effects of mole changes.

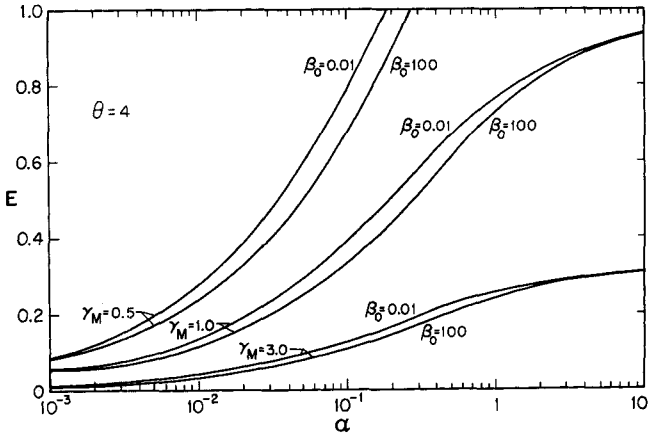

Fig. 6. Effectiveness factor in the transition region for slab geometry showing the effects of changes in the flow parameter.

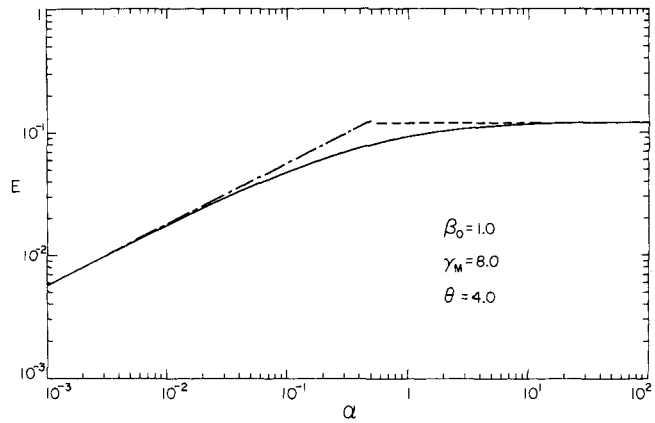

Fig. 7. Effectiveness factor predicted by the dusty-gas model (solid curve) for slab geometry compared with the usual molecular and Knudsen models (dashed curves).

to be completely dominated by molecular diffusion under constant external pressure, the pressure parameter α for the system conditions should be greater than 10^4.

Even for mole changes corresponding to $\theta = 4$ the pressure profile is essentially constant inside the pellet. This interesting result, which is not intuitively obvious, can be explained on the basis that the slip-flow term in the flux equation is large enough to accommodate the backflow of excess moles produced by the reaction. This same argument also explains why the effectiveness factor is independent of β_0.

We should point out that, since the pressure on the external surface of each pellet is constant, there is no net mass flux at the pellet boundaries and hence no hydrodynamic velocity. This is also the case inside the pellet.

Finally, if an overall pressure gradient were imposed across the pellet, there would be net mass flux through the pellet resulting in a hydrodynamic velocity gradient. Under these conditions, the effectiveness factor would be affected by D'Arcy flow and hence would be a function of the flow parameter, β_0.

Knudsen Regime

In agreement with Otani et al. (1964), the effectiveness factor is a unique function of the Thiele modulus γ_K defined in terms of the Knudsen diffusivity. This means that it is completely independent of the other four parameters including θ, which is an indicator of mole changes. Hence, the E versus γ_K curve in the Knudsen regime is precisely the same as the E versus γ_M curve for $\theta = 1$ in the molecular regime. For intrapellet transport to be completely dominated by Knudsen diffusion, the pressure parameter α for the system conditions should be less than 10^{-4}.

The pressure profile inside the pellet for external isobaric conditions is a function of θ as well as y_{AL} and, for the case studied here, is very significant. For $y_{AL} = 1$, as used throughout this study, the dimensionless pressure ξ increases toward the pellet center-plane and finally reaches an asymptotic value equal to $\sqrt{\theta}$.

Although no viscous flow can exist under Knudsen conditions in a porous solid, the transport of molecules requires fugacity gradients which in this case manifests itself in partial pressure gradients existing within the porous structure. For the case of increasing moles with extent of reaction, the summation of the partial pressures (total pressure) of the diffusing species increases toward the center of the pellet. This is required by the system in order to expel the excess moles in the reaction. Again, these results are not intuitively obvious.

Transition Region

The transition region often dominates under catalyst conditions used in many industrial operations. Here it is found that the effectiveness factor is a function of all five dimensionless quantities α, β_0, θ, γ_M, and y_{AL} which are considered the main parameters in this study. In Figure 7, extensions of the purely molecular and purely Knudsen models into the transition region are compared with the E versus α locus predicted by the extended dusty-gas model for fixed $\gamma_M = 8.0$, $\beta_0 = 1.0$, and $\theta = 4$ in slab geometry. Within the range of $10^{-2} < \alpha < 10^{+1}$, the deviation of the simpler models from the extended dusty-gas model is significant but is not particularly significant outside that range. For decreasing values of γ_M and for the other geometries, the deviations occur over a broader range than that shown in Figure 7; for this reason, the transition region broadly exists in the range of $10^{-4} < \alpha < 10^4$.

For a pellet with isobaric external conditions, the effect of the flow parameter β_0 is only important in the transition region, and here its major effect is bracketed between β_0's of 10^{-2} to 10^2 for each value of α, which in turn ranges from 10^{-2} to unity. Outside these rough upper and lower limits for α and β_0, the effect of β_0 is not important.

As in the case of Knudsen-dominated transport, the pressure profile varies significantly inside the pellet but to a lesser extent. In contrast to the case of molecular-diffusion transport, the slip-flow and D'Arcy terms in the transport equation both contribute to the backflow of excess moles inside the pellet.

We should like to point out in conclusion that use of the extended dusty-gas model in this general treatment has the added advantage of not requiring information about the pore-size distribution in the catalyst pellets. A simple experimental determination of the extended dusty-gas constants C_0, C_1, and C_2 is all that one needs in using the model. A detailed paper on the experimental determination of these constants will soon appear.

Many of the generalizations in this study should be applicable to higher order reactions as well as to nonisothermal conditions. Future papers will consider these matters in detail.

ACKNOWLEDGMENT

The authors acknowledge the National Science Foundation for support of this work under NSF Grant GK 25570.

NOTATION

a, a' = grouping terms defined by Equations (3) and (6), respectively, g-mole/cm-s
A = component A
b, b' = grouping of terms defined by Equations (4) and (7), respectively, g-mole-cm/dyne-s
B = component B
C_0 = constant dependent only upon structure of porous medium and giving relative D'Arcy flow permeability, cm^2
C_1 = constant dependent only upon structure of porous medium and giving relative Knudsen flow permeability, cm
C_2 = constant dependent only upon structure of porous medium and giving ratio of molecular diffusivity within the porous medium to the free gas diffusivity, dimensionless
D_{AB} = free gas mutual diffusivity in a binary mixture of components A and B, cm^2/s
D^0_{AB} = $D_{AB}P$, dynes/s
E = effectiveness factor defined by Equation (36), dimensionless
f = grouping of terms defined by Equation (12), g-mole/cm-s
j = geometric constant having values of 1, 2, and 3 for an infinite slab, cylinder, and sphere, respectively
k = zero-order rate constant based on unit volume of catalyst, g-mole/cm^3-s
k' = zero-order rate constant based on unit surface area of catalyst, g-mole/cm^2-s
K_A = Knudsen effective diffusivity = $C_1\sqrt{R_gT/M_A}$, cm^2/s
K_m = $y_BK_A + y_AK_B$, cm^2/s
L = radial distance from the center for spheres, from the center line for cylinders and from the center plane for slabs to the exterior surface of the catalyst pellet, cm
M = molecular weight, g/g-mole
n = flux ratio = $\vec{N}_B/\vec{N}_A = -(M_A/M_B)$
$\vec{N}$ = molar flux, g-moles/cm^2-s
P = total pressure, dynes/cm^2
P_L = total pressure at the same position as taken for y_{AL}; that is, the exterior of the pellet, dynes/cm^2
Q = lumped dependent variable defined by Equation (32), dimensionless
R = lumped dependent variable defined by Equation (33), dimensionless
R_g = gas constant, 8.31×10^7 ergs/g-mole-°K
S = surface area of exposed catalyst, cm^2/g
T = absolute temperature, °K
V = grouping of terms defined by Equation (34), dimensionless
W = grouping of terms defined by Equation (35), dimensionless
X = dimensionless distance in the pellet defined by Equation (26)
X_0 = dimensionless distance in the pellet at which the concentration of A becomes zero
X^* = ratio defined by Equation (31)
y = mole fraction
y_{AL} = mole fraction of component A at the external face of the pellet
Y = mole fraction ratio defined by Equation (25)
Z = distance in direction of mass transfer, cm
Z_0 = distance from the center plane of the pellet at which the concentration of A becomes zero, cm

Greek Letters

α = dimensionless main parameter defined by Equation (18)
β = dimensionless auxiliary parameter defined by Equation (23)
β_0 = dimensionless main parameter defined by Equation (19)
γ_K = dimensionless auxiliary parameter defined by Equation (22) and called Knudsen Thiele modulus
γ_M = dimensionless main parameter defined by Equation (20) and called molecular Thiele modulus
θ = dimensionless main parameter defined by Equation (21)
μ = viscosity, g/cm-s
ξ = dimensionless pressure defined by Equation (28)
ρ = density, g/cm^3

Subscripts

A = component A
B = component B
K = Knudsen
L = at exterior pellet face
m = mixture
M = molecular
p = pellet

LITERATURE CITED

Aris, R., "On Shape Factors for Irregular Particles I. The Steady State Problem. Diffusion and Reaction," *Chem. Eng. Sci.*, **6**, 262 (1957).

Bischoff, K. B., "Effectiveness Factors for General Reaction Rate Forms," *AIChE J.*, **11**, 351 (1965).

Evans, II, R. B., G. M. Watson, and E. A. Mason, "Gaseous Diffusion in Porous Media at Uniform Pressure," *J. Chem. Phys.*, **35**, 2076 (1961).

Gunn, R. D., and C. J. King, "Mass Transport in Porous Materials under Combined Gradients of Composition and Pressure," *AIChE J.*, **15**, 507 (1969).

Lin, K., and M. M. Lih, "Concentration Distribution, Effectiveness Factor and Reactant Exhaustion for Catalytic Reaction with Volume Change," *ibid.*, **17**, 1234 (1971).

Mason, E. A., A. P. Malinauskas, and R. B. Evans, "Flow and Diffusion of Gases in Porous Media," *J. Chem. Phys.*, **46**, 3199 (1967).

Otani, S., N. Wakao, and J. M. Smith, "Intrapellet Pressure Gradients in Porous Catalysts," *AIChE J.*, **10**, 130 (1964).

Smith, N. L., and N. R. Amundson, "Intraparticle Diffusion in Catalytic Heterogeneous Systems," *Ind. Eng. Chem.*, **43**, 2156 (1951).

Thiele, E. W., "Relation between Catalytic Activity and Size of Particle," *Ind. Eng. Chem.*, **31**, 916 (1939).

Wakao, N., and J. M. Smith, "Diffusion and Reaction in Porous Catalysts," *Ind. Eng. Chem. Fundamentals*, **3**, 123 (1964).

Weekman, V. W., Jr., and R. L. Gorring, "Influence of Volume Change on Gas-Phase Reactions in Porous Catalysts," *J. Catal.*, **4**, 260 (1965).

Wei, J., "Intraparticle Diffusion Effects in Complex Systems of First Order Reactions I. The Effects of Single Particles," *ibid.*, **1**, 526 (1962).

Weisz, P. B., and C. D. Prater, "Interpretation of Measurements in Experimental Catalysis," *Advan. Catal.* **6**, 143 (1954).

Wheeler, A., "Reaction Rates and Selectivity in Catalyst Pores," *ibid.*, **3**, 249 (1951).

Youngquist, G. R., "Diffusion and Flow of Gases in Porous Solids," *Ind. Eng. Chem.*, **62**, 52 (1970).

Manuscript received June 5, 1972; revision received and accepted January 29, 1973.